

# Brownian Motion Captured with a Self-Mixing Laser

**Kenju Otsuka, Yoshihiko Miyasaka, Seiichi Sudo,  
Natsumi Sano and Hironori Makino**

Department of Human and Information Science, Tokai University  
1117 Kitakaname, Kanagawa, 259-1292 Japan

## Abstract

We report on our successful real-time measurement of the dynamic frequency-shift of light by particles in Brownian motion through self-mixing laser spectroscopy with extreme optical sensitivity. We demonstrated successful particle sizing and calculating particle-size distributions from modulated power spectra. From the demodulated signals, it was found that the changes over time in the non-stationary random walks of small particles suspended in water result in different averaged dynamics when the field of vision for particles seen by the laser beam (scale of the observation) is changed. At a small focal volume of the laser beam, in which the relevant diffusion broadening is observed, the averaged motion which can be represented by the motion of a "virtual" single particle, whose velocity possesses a Gaussian-white property. The average motion is found to constitute stationary fluctuations, featuring random sequences of the Lorentz-type spectrum and double-peaked probability distribution function for displacements.

**Keywords:** Microchip solid-state laser, Self-mixing modulation, Brownian motion, Particle sizing

## 1. Introduction

In disciplines ranging from fluids through ecosystems, chemistry, and electronics to finance systems, we find phenomena associated with non-Gaussian intensity probability distribution functions that have 'long tails' or reflect 'self-similar' (i.e., non-stationary) processes. This family of distributions was discovered by Levy [1] and shown to be applicable to very many phenomena in a broader new interdisciplinary field by Mandelbrot [2]. This paper deals with a novel approach to the measurement and presentation of one such phenomenon discovered in small particles in Brownian motions, that is the prototypical example which exhibits non-stationary behavior, i.e., random walk. Our motivation behind this study is to capture an intriguing dynamic behavior of Brownian particles, which appears as an averaged motion of independent random walks depending on the scale of observation. Such a study would provide a conceptually new insight into the general Brownian motions.

The coherent nature of laser light has been applied in dynamic light-scattering (DLS) method [3] for characterizing motions of small particles in suspension, including gasses, liquids, solids, and biological tissue [4-6]. DLS approach toward measuring diffusion broadening of scattered light from moving small particles, is helpful to extract useful information on particles in Brownian motions and particle sizing. In conventional DLS, there are two methods: In the first method, an intensity fluctuation of scattered light passing through a small pin-hole, which represents beat signals of Doppler-shifted fields scattered by different particles, is measured. Then, an autocorrelation function is calculated from long-term experimental time series. From the calculated autocorrelation

function, the distribution of particle sizes can be analyzed. In the second method, beat signals between a local oscillator light field and a scattered light field are measured using an optical interferometer, in which a frequency shifter is introduced in one arm to create the frequency-shifted field while the unshifted beam in another arm acts as a local oscillator field. In this heterodyne detection scheme, the spectral broadening is measured by a spectrum analyzer [7].

On the other hand, we developed so far the real-time nanometer vibration measurement system with extreme optical sensitivity using microchip solid-state lasers. In this scheme, the laser itself is intensity-modulated by beat signals between a lasing field (i.e., unshifted local oscillator) and a frequency-shifted scattered field through the interference of two fields [8,9]. So, we do not need an optical interferometer and furthermore high optical sensitivity is ensured due to the enhanced self-mixing modulation effect which is proportional to large fluorescence-to-photon lifetime ratios in microchip lasers. Therefore, this self-aligned self-mixing photon correlation spectroscopy using backscattered light is expected to make easy particle sizing possible and give us a way to capture the averaged motion of particles in real-time, each of which independently scatters the laser light. The distinct advantage of our self-mixing scheme is that we can demodulate the laser intensity fluctuations through a simple frequency-modulated (FM)-wave demodulation circuit [8,9].

In this paper, we demonstrate that quick particle sizing and determining distribution of size of particles in suspension are possible from analyses of power spectra of modulated signals exhibiting diffusion broadening obeying the Einstein-Stokes relation. From demodulated signals, it is shown that when the field of vision

of particles by the laser beam is adjusted such that the relevant diffusion broadening is observed, stationary fluctuations featuring random sequences possessing Lorentz type of power spectrum appear in the averaged movement of individual particles in non-stationary random walks. We observed non-Gaussian, but stationary displacement probability distributions and successfully captured the sound of such averaged motions.

## 2. Self-mixing laser photon-correlation spectroscopy of Brownian particles

### 2.1 Experimental setup of self-mixing laser spectroscopy of Brownian particles

The experimental setup is shown in Fig. 1, which is similar to that used in refs. [8,9]. The laser was a laser-diode (LD) pumped 0.3-mm-thick LiNdP<sub>4</sub>O<sub>12</sub> (LNP) laser with a coating of mirror on each end and operating at the wavelength of  $\lambda = 1048$  nm. The collimated beam from the LD (wavelength:  $\lambda_p = 808$  nm) was passed through a pair of anamorphic prisms and then focused on the LNP crystal by a microscope objective lens. The greater portion (96 %) of the output light was passed through an iris, frequency-shifted by two acousto-optic modulators (AOMs), and then delivered to the scattering cell. The fused quartz cell was filled with water that contained spherical polystyrene latex particles (STADEx: at 1% density).

Microscope objective lenses with different numerical apertures (NA = 0.25, and 0.4) were used to focus the laser beam such that the

focal plane (beam waist) was within the cell, where a depth from the cell's inner surface (wall),  $d$ , was varied. The quartz cell's surface was slightly tilted to suppress the light feedback from the surface. Changing the modulation frequencies of the up-shift and down-shift AOMs produced a shift in optical carrier frequency of  $2f_s = 2$  MHz at the end of the roundtrip. The rest (4 %; 80  $\mu$ W) of the output light was detected by an InGaAs photoreceiver (New Focus1811: DC-125 MHz), and the electrical signal produced by this device was fed to further electronic devices; rf spectrum analyzer (Tektronix 3026: DC-3GHz), digital oscilloscope (Tektronix TDS 540D: DC-500 MHz), and FM receiver. The laser's threshold level of pump power was 30 mW and its slope efficiency was 40 %.

### 2.2 Lorentz broadening and particle sizing

The self-mixing effect is produced by interference between the laser field and the Doppler-frequency-shifted field fed back from the moving particles to the laser; this led to intensity modulation of the laser at the beat frequency between the two fields [8,9]. The short-cavity configuration of our thin-slice solid-state laser led to a photon lifetime six orders of magnitude shorter than the 120- $\mu$ s fluorescence lifetime. This compensates for the extremely weak optical feedback condition and gives us a means for the real-time examination of dynamic light scattering by particles in Brownian motion; that is, detection of the frequency-modulation-driven variations in the intensity of the output laser light at beat frequencies between a lasing (i.e., unshifted local oscillator) and scattered fields from particles,  $2f_s + f_D(t)$ , the carrier frequency of which is  $2f_s = 2$  MHz as indicated in Fig. 1.

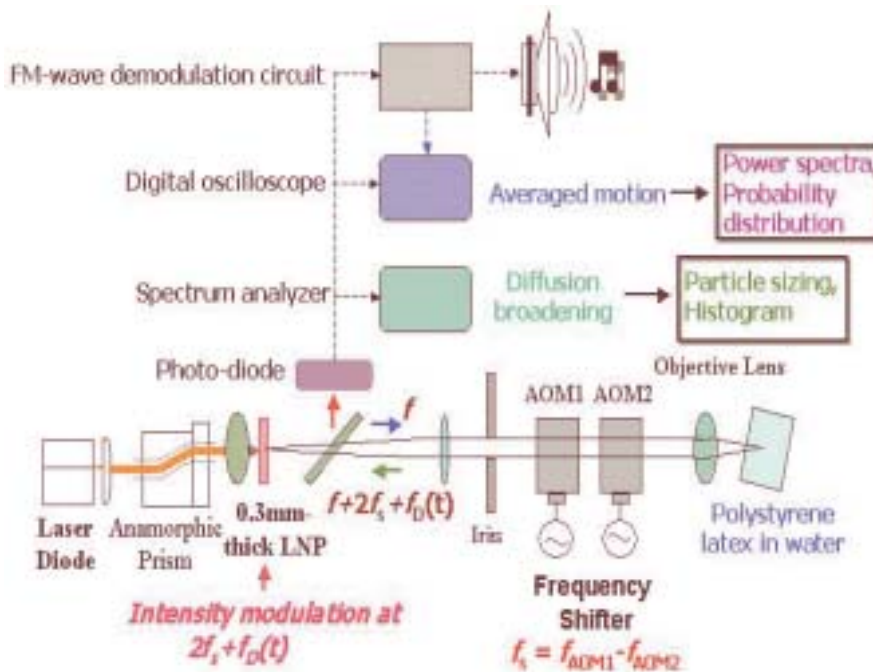


Fig.1. Experimental setup. PD: photodiode, SA: spectrum analyzer, DO: digital oscilloscope, FMD: FM demodulation circuit.

Figure 2(a) shows an example of modulated output waveforms, with a magnified view of the waveform shown as the inset, where 207-nm-diameter particles were used. Note that a large fluctuation in the envelope of the 2-MHz carrier wave amplitude is a result of the fluctuation over time in the number of particles coming in and out of the region on which the laser beam is focused, since the modulation depth (i.e., feedback ratio) depends on the number of scattering particles. Let us examine power spectra of modulated signals. In Fig. 2(b) show power spectra obtained for 107-nm, 207-nm, and 458-nm

We could perform an excellent particle sizing for diluted sample with a 0.01% particle density with the present self-mixing laser.

### 2.3 Distribution of particle sizes

We have performed successful evaluations of *average* diameters of polystyrene latex spheres of different diameters (107 nm, 207 nm and 458 nm) within 5% accuracy by averaging of many (e.g., 100)

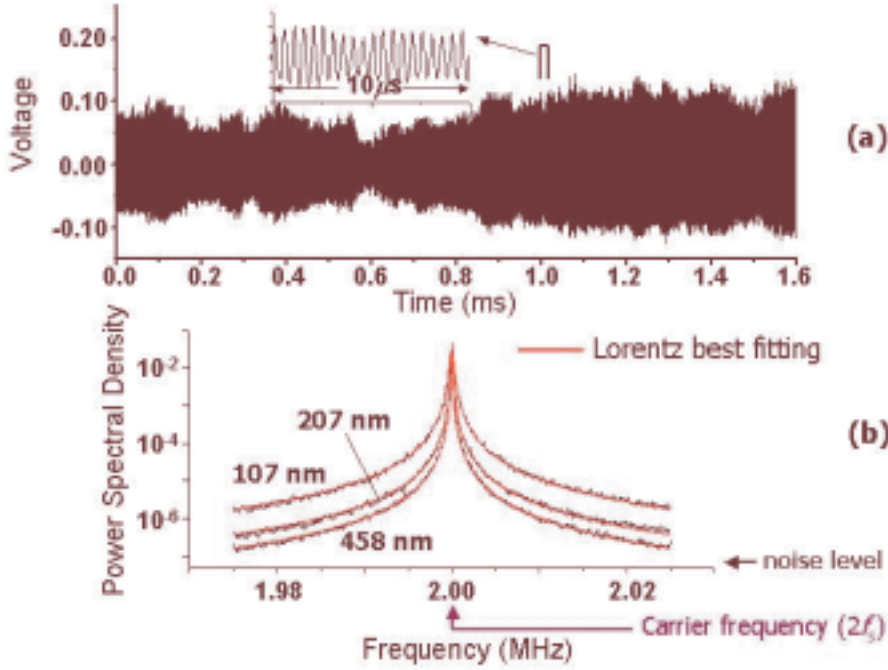


Fig. 2 Modulated signals. (a) Intensity wave form for 207-nm particles. (b) Power spectra for different diameter particles measured with a microscope objective lens of NA = 0.25.

particles, where a microscope objective lens of NA = 0.25 was used. Each power spectrum was obtained by averaging 100 traces from the spectrum analyzer.

It is well known that the frequency spectrum of the light scattered by a Brownian particle show the Lorentz profile [3] according to the fluctuation-dissipation theorem. When each particle is moving independently and the scattered field amplitude from each particle is constant, the power spectral densities of modulated signals shown in Figs. 2(b) are expected to be fitted by the following Lorentz curve similar to that in the case of heterodyne detection using interferometer [7]:

$$I(k, \omega) = A + B(k^2 D) / [(\omega - 4\pi f_s)^2 + (k^2 D)^2], \quad D = k_B T / 3\pi\eta a \quad (1)$$

Here,  $D$  is diffusion constant,  $a$  is the diameter of the Brownian particles,  $\eta$  is the liquid medium's coefficient of viscosity,  $k_B T$  is Boltzmann's factor, and  $k$  is the wave vector. The observed rf power spectrum provides a good representation of the frequency spectrum of laser light scattered by independent particles in Brownian motion. The half-width at half-maximum frequency width,  $(4\pi a / \lambda)^2 D \sin^2(\theta/2)$  ( $\theta$ : scattering angle;  $\theta = \pi$  in our case), as estimated from the Lorentzian curve of best fit obtained by the fitting software shown in Fig. 2(b), yielded the particle diameter of 103 nm, 203 nm and 420 nm for different particles, respectively.

power spectra of modulated signals like Fig. 2(b). Here, let us discuss about measurement of particle distributions by using the present self-mixing scheme.

From FFT (Fast Fourier Transformation) of averaged one-side power spectra of modulated signals, we calculated the “net” normalized second-order autocorrelation function  $G^{(2)}(\tau)$  which is related to the first-order autocorrelation function  $g^{(1)}(\tau)$  through Siegert relation as [10]:

$$g^{(1)}(\tau) = \int G(\Gamma) \exp(-\Gamma\tau) d\Gamma = [G^{(2)}(\tau)]^{1/2} \quad (2)$$

$$G^{(2)}(\tau) = [g^{(2)}(\tau) - C] / \beta, \quad (3)$$

with  $G(\Gamma)$  being the normalized distribution of linewidth.  $C$  is the background which can be measured at large delay times  $\tau$ . We assume  $\beta$  to be an unknown parameter in the data fitting procedure. The “net” signal autocorrelation function  $G^{(2)}(\Gamma)$  calculated from the averaged power spectrum for 207-nm particles is shown in Fig. 3(a). By using the histogram method [10], we calculated the distributions of linewidth  $G(\Gamma)$  and particle size from  $G^{(2)}(\Gamma)$ . Results are shown in Figs. 3(b) and 3(c), respectively, where the averaged particle size was 204 nm. Similar results were obtained for particles of 107-nm and 458-nm diameters.

We are now developing a statistical analysis tool for calculating a histogram of particle sizes directly from a measured power spectrum especially for mixed particles with different sizes.

### 3. Stationary fluctuation in demodulated signals

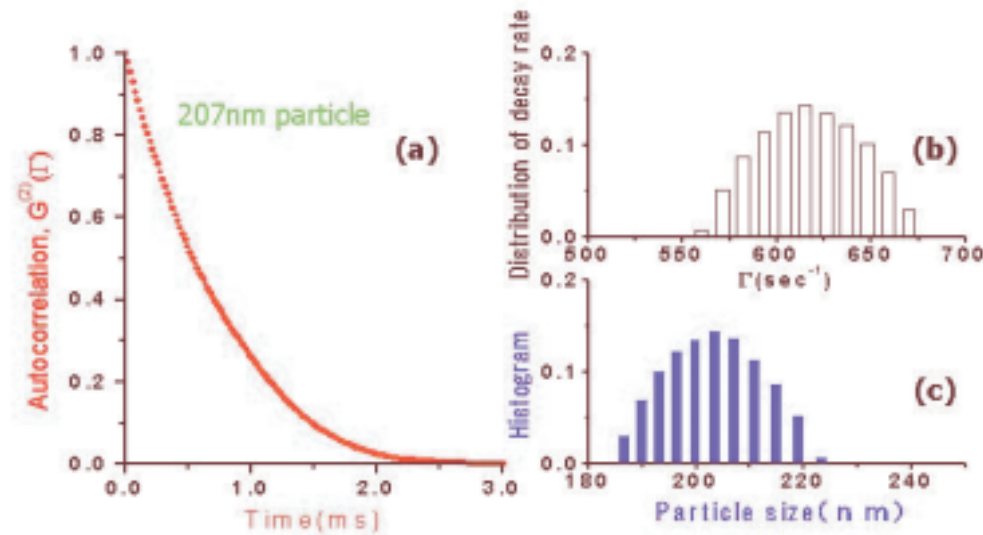


Fig. 3. (a) Normalized “net” autocorrelation function  $G^{(2)}(\tau)$  calculated from the averaged power spectrum of modulated signal for 207-nm polystyrene latex in water assuming  $\beta = 1$ . (b) Probability distribution of linewidths  $G(\Gamma)$ . (c) Histogram of particle sizes.

#### 3.1 Random sequence of Lorentz-type spectrum

Next, let us investigate an averaged motion of Brownian particles within the scale of observation by the laser beam by demodulating the laser output intensity. A demodulated signal voltage,  $V_o(t)$ , is considered to be proportional to the displacement of a single “virtual” particle along the laser axis,  $D_p(t)$ , whose instantaneous velocity is given by the average of instantaneous velocities along the laser axis of individual particles, each of which has its own velocity vector over times. A super-heterodyne method with a central

frequency of 10.7 MHz was employed in FMD in Fig. 1 to demodulate the FM wave; the amplifier had a gain of 20 dB and a 3-dB bandwidth of 111 kHz. An example demodulated output voltage is shown in Fig. 4(a), in which the displacement is related to the output voltage as  $D_p/V_o = 5$  [nm/mV]. To obtain such a voltage-displacement relationship, we used Hilbert transformation of the modulated output waveform and phase-sensitive detection in the

PC, assuming the relation  $D_p(t) = \lambda \Delta\Phi(t)$ , where  $\Delta\Phi$  is the phase difference between the 2-MHz carrier (reference) wave and the modulated wave, as calculated from Gabor’s analytic signal [8,9].

Note that the autocorrelation function and the corresponding power spectral density exhibit an exponential decay and random sequences possessing Lorentz type of spectrum, as shown in Figs. 4(b) and (c), respectively where the curves of best fit are indicated.

The roll-off point from the  $f^0$ -type toward the asymptotic  $f^{-2}$  behavior is found to shift to the low-frequency side with increasing

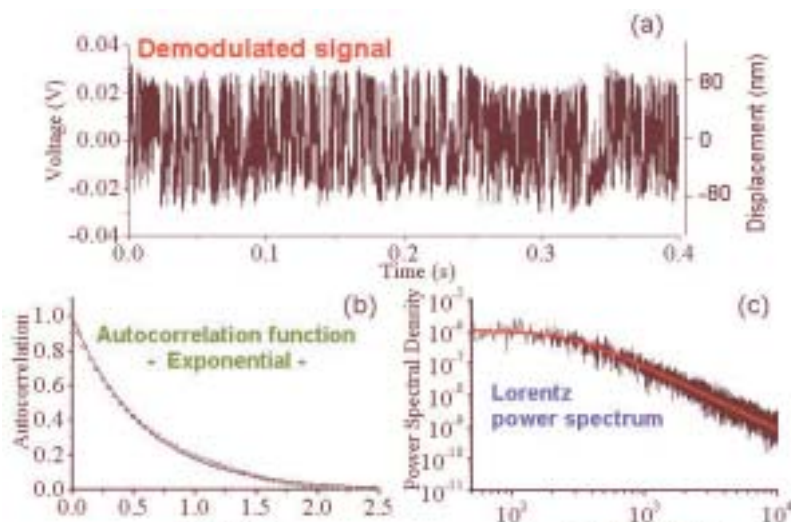


Fig.4. Demodulated signals. (a) Intensity waveform for 207-nm particles. (b) Autocorrelation function. (c) Power spectrum

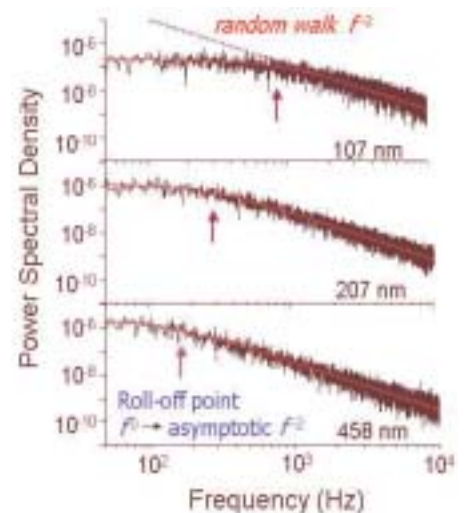


Fig. 5. Random sequence of Lorentz-type spectrum for averaged motions of Brownian particles with different sizes.

the diameter of particles in suspension as shown in Fig. 5.

We could successfully captured a 'sound' of the averaged motion of Brownian particles from the demodulated signal.

### 3.2 Probability Distribution of Averaged Displacement and Velocity

In connection to such averaged Brownian motion of particles within the scale of observation, we examined a long-term intensity probability distribution of the demodulated output intensity which corresponds to the averaged displacement. Example results for particles with different diameters are shown in Fig. 6(a). The output voltage fluctuation (i.e., dynamic displacement of a single "virtual" particle) indicates stationary intensity probability distributions featuring double peaks. While the Langevin equation for a single Brownian particle tells us that the displacement probability distribution is non-stationary.

Note that low-frequency fluctuation components exhibiting the asymptotic  $f^0$  property in Lorentz power spectra were found to contribute predominantly to the double-peak nature inherent in the probability distribution functions shown in Fig. 6(a). It should be noted that velocity probability distribution function calculated from temporal evolutions of displacement always exhibits Gaussian distribution similar to a Brownian particle, however, power spectra of temporal evolutions of velocity of such a "virtual" particle shows  $f^0$  property as shown in Figs. 6(b)-(c). Table I summaries statistical

properties of motions of a "virtual" particle discussed above in comparison with those of a single Brownian particle that were confirmed by numerical simulation of the Langevin equation. A "virtual" particle possesses a Gaussian-white type property in its velocity and a stationary Lorentz type property in its displacement, while a single Brownian particle possesses well-known Gaussian-Lorentz and nonstationary  $f^{-2}$  type properties in its velocity and displacement.

Finally, the effect of the field of vision of particles by the laser beam was briefly examined. With increasing a beam-waist diameter  $D_0$  larger than  $100\ \mu\text{m}$  by using a conventional lens, the diffusion broadening in the modulated output was suppressed as shown by black curve in Fig. 7(a), in which the demodulated output voltage was extremely small and the sound was unheard: the Lorentz-type power spectrum and double-peaked distribution function were not observed in the demodulated output, as shown in Figs. 7(b) and 7(c). Here, the correct Lorentz broadening obtained for 207-nm particles with the objective lens of  $\text{NA}=0.4$  is shown by red curve in Fig. 7(a) for comparison. In DLS, in general, an effective symmetric plane-wave scattering with respect to the focal plane occurs within the focused beam region, i.e., focal depth  $f_D = \lambda/2(\text{NA})^2$  [6]. In the case of a conventional lens with small NA, the focal depth becomes larger. Therefore, light is scattered multiple times by particles before re-injection into the laser and consequently details of particle dynamics are considered to be lost [6].

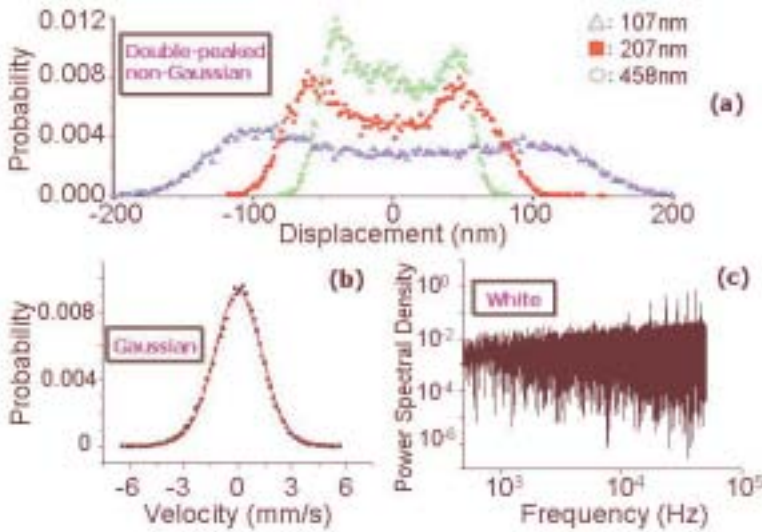


Fig. 6. Characteristics of demodulated outputs. (a) Displacement probability distribution of a virtual particle. (b) Velocity probability distribution of a virtual particle. (c) Power spectrum of temporal variation of the velocity of a virtual particle. (b) and (c) are results obtained for 207-nm particles.

**TABLE I. Statistical properties of motions of a Brownian particle and the virtual particle. PD: probability distribution, PS: power spectrum**

Particle	Displacement (PD-PS)	Velocity (PD-PS)
Brownian particle	Nonstationary - $f^{-2}$	Gaussian - Lorentz
Virtual particle	Stationary - Lorentz	Gaussian - white

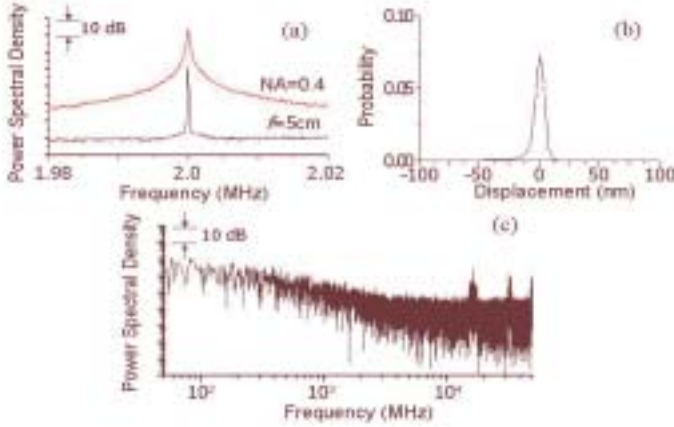


Fig. 7. Results for 207-nm particles obtained by using a 5-cm focal-length lens to focus the beam. (a) Power spectrum of the modulated signal. (b) Probability distribution of the displacement. (c) Power spectrum of demodulated output. The red curve in (a) obtained with the microscope objective lens of NA = 0.4 is shown for comparison..

#### 4. Discussion on double-peaked probability distributions of demodulated signals

Let us discuss about the double-peaked intensity probability distribution shown in Fig. 6(a) employing a statistical analysis for many particles. Such distributions are considered to arise when multiple particles within the focused beam region, where an effective plane-wave scattering occurs [6], can move symmetrically (i.e., the field of vision for particles is symmetric) with respect to the focal plane.

In this case, the distribution function of the velocity component along the laser axis  $V_x$  for a single particle is given by

$$f(V, V_x) = (1/\pi)(V^2 - V_x^2)^{-1/2} \quad (4)$$

where  $V$  is the absolute value of the velocity and  $|V_x| \leq V$ . Since this function has singular points at  $V_x = \pm V$ , it is convenient to use its cumulative distribution function

$$C(V, V_x) = 2 \int_0^{V_x} f(V, \sigma) d\sigma \quad (5)$$

The ensemble average is expressed by

$$\langle C(V_x) \rangle = 4\pi(\alpha/\pi)^{3/2} \int_{V_x}^{\infty} V^2 \exp(-\alpha V^2) C(V, V_x) dV \quad (6)$$

assuming a Maxwell distribution for  $V$ , where  $\alpha = m/2k_B T$  ( $m$ : mass of the particle). When  $\langle C(V_x) \rangle$  is differentiable, the ensemble average of the velocity distribution function is given by  $\langle f(V_x) \rangle = d\langle C(V_x) \rangle / dV_x$ . Calculated velocity probability distribution functions for particles of different diameters are shown in Fig. 8.

Double-peaked distribution functions, which are found to be of similar shape of observed displacement probability distribution functions, are obvious, in which peaks approaches  $V_x = 0$  with increasing the particle size, i.e., mass, similar to Fig. 6(a). This correspondence suggests that there exist some simple scaling relation between the two distribution functions when the observation time is large enough. In our experiment with microscope objectives, "tails" in the velocity (i.e., overall displacement) distribution functions are considered to be suppressed, with the measurable displacement being limited by the scale of observation, i.e., the size of focus region. Indeed, a simple truncation of  $V$  resulted in the

suppression of tails as expected. It should be noticed that the calculated velocity distribution function is different from the Gaussian probability distribution of a single "virtual" particle shown in Fig. 6(b).

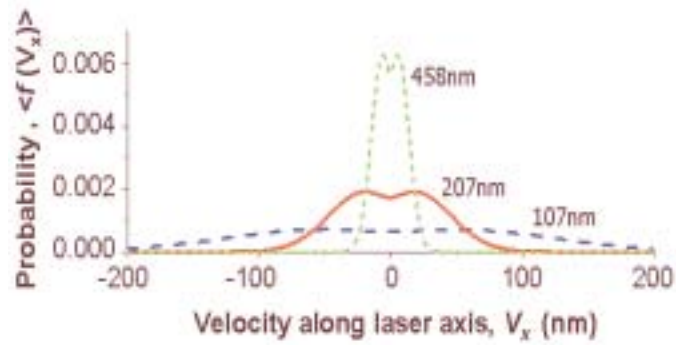


Fig. 8. Probability distribution of velocities along the laser axis of many particles in the symmetric plane-wave scattering regime.

#### 5. Summary

In summary, we have demonstrated successful characterization of particle sizes and their distribution by self-mixing laser spectroscopy with extreme optical sensitivity. From demodulated signals we found that the averaged motion of many Brownian particles in suspension can be described by a single "virtual" particle motion whose velocity obeys a Gaussian-white property, exhibiting random sequences possessing the Lorentz-type of spectrum and inherent double-peaked displacement probability distributions.

The theoretical study of multiple-particle dynamics, which depend on the field of vision for particles seen by the laser beam, would provide conceptually new insights into general Brownian: it could be done by numerical simulation of the self-mixing laser equation coupled with spatio-temporal stochastic differential equations for velocities of individual particles, including independent Langevin forces.

The extreme optical sensitivity of the form of self-mixing laser Doppler vibrometry setup would make it applicable to a wide range of targets for investigating averaged dynamics of spatially extended many-body systems under different scales of the observation. They include free electrons in solids and plasma, atoms, molecules and biological specimens and in general, targets distributed in diffusive media.

---

## References

1. P. Levy., Random functions: General theory with special reference in Laplacian random functions, *University of California Publications in Statistics* **1**, 331-390 (1953)..
2. B. B. Mandelbrot, *The Fractal Geometry of Nature* (Freeman, San Francisco, 1982).
3. B. J. Berne and R. Pecora, *Dynamic Light Scattering* (John Wiley and Sons, New York, 1976).
4. H. Z. Cummins, N. Knable, and Y. Yeh, "Observation of diffusion broadening of Rayleigh scattered light," *Phys. Rev Lett.* **12**, 150-153 (1964).
5. R. C. Youngquist, S. Carr, and D. E. N. Davies, "Optical coherence-domain reflectometry: a new optical evaluation technique," *Opt. Lett.* **12**, 158-160 (1986).
6. D. A. Boas, K. K. Bizheva, and A. M. Siegel, "Using dynamic low-coherence interferometry to image Brownian motion with highly scattering media," *Opt. Lett.* **23**, 319-321 (1998).
7. M. Harris, G. N. Pearson, C. A. Hill, and J. M. Vaughan, "The fractal character of Gaussian-Lorentzian light," *Opt. Commun.* **116**, 15-19 (1995).
8. K. Otsuka, K. Abe, J.-Y. Ko, and T.-S. Lim, "Real-time nanometer-vibration measurement with a self-mixing microchip solid-state laser," *Opt. Lett.* **27**, 1339-1341 (2002).
9. K. Abe, K. Otsuka, and J.-Y. Ko, "Self-mixing laser Doppler vibrometry with high optical sensitivity: application to real-time sound reproduction, " *New J. Phys.* **5**, 8.1-8.9 (2003).
10. E. Gulari, G. Erdogan, Y. Tsunashima, and B. Chu, "Photon correlation spectroscopy of particle distribution," *J. Chem. Phys.* **70**, 3965-3972 (1979).